# $^{13}C$ Knight shift in TTF-TCNQ($^{13}C$): Determination of the local susceptibility*

E. F. Rybaczewski,† L. S. Smith, A. F. Garito, and A. J. Heeger
*Department of Physics and the Laboratory for Research on the Structure of Matter, University of Pennsylvania, Philadelphia, Pennsylvania 19174*

B. G. Silbernagel
*Exxon Research and Engineering Company, Linden, New Jersey 07036*

(Received 28 April 1976)

The temperature dependent $^{13}C$ Knight shift and spin-lattice relaxation rate of tetrathiafulvalene-tetracyanoquinodimethane (TTF-TCNQ) labeled at the CN group of TCNQ are presented. The Knight shift is a direct measure of the time-averaged local susceptibility on the TCNQ chain. From these data, the local susceptibilities on the TTF and TCNQ chains are obtained. The TCNQ chain susceptibility falls to zero below 54 K, indicating the onset of long-range order. The TTF susceptibility persists to lower temperature decreasing below approximately 49 K. The temperature dependence of the TCNQ chain susceptibility is in quantitative agreement with the calculated susceptibility based on the Peierls-Fröhlich model with a complex order parameter for $T > 54$ K which becomes pinned below 54 K. The susceptibility and thus the density of states on the TTF chain is considerably larger (a factor of 2 at 300 K) than that of the TCNQ chain suggesting a correspondingly narrower bandwidth.

## I. INTRODUCTION

The organic charge-transfer salt tetrathiafulvalence-tetracyanoquinodimethane (TTF-TCNQ) is a one-dimensional (1D) metal[1] at high temperatures. A series of dc electrical transport,[2-4] microwave,[5-7] and optical studies[8-13] confirm the 1D properties and show TTF-TCNQ undergoing a transition below 54 K to a high-dielectric-constant[5,6] semiconductor state.

Earlier, it was suggested[3,14] that the behavior of TTF-TCNQ is associated with the Peierls instability[15,16] of the 1D metallic system in which a phonon mode is driven soft[17] by the divergent response of the electron gas at $q = 2k_F$. The subsequent observation of an incommensurate superlattice at low temperatures using diffuse x-ray[18,19] and elastic-neutron-scattering[20] techniques confirmed the existence of the Peierls instability and the charge-density-wave (CDW) ground state in TTF-TCNQ, with the magnitude of $2k_F$ equal to $0.295b^*$ and thus a partial charge transfer of 0.59 electrons per donor-acceptor pair. Evidence of the giant Kohn anomaly associated with the dynamic Peierls distortion above 54 K has been obtained from x-ray[18,19] and inelastic-neutron-scattering[21,22] studies.

TTF-TCNQ crystallizes in regular segregated stacks of TTF cations (holes) and TCNQ anions (electrons).[23] Experimentally, the partial charge transfer, the localization on individual chains as indicated by the diffuse perpendicular transport,[5] the observation of multiple structural transitions,[18-20,24,25] and the results of alloy studies[26] suggest that different electronic properties might be expected for the TTF-hole and TCNQ-electron chains. Moreover, the shear forces which elastically couple the TTF and TCNQ chains have been shown to be weak.[27] Recently, Rice *et al.*[28] have presented theoretical arguments that the coupling to the various intramolecular modes plays a major role in stabilizing the Peierls state in 1D conductors. Thus, the different intramolecular mode structure for the TTF and TCNQ molecules will result in different effective electron-phonon coupling constants for the two subsystems.

Earlier studies of the individual chain properties have revealed differences in the local chain magnetic susceptibilities. Proton nuclear magnetic relaxation studies[29] on selectively deuterated samples of TTF-TCNQ demonstrated different relaxation rates for the two chains. Studies of the $g$ value[30] and linewidth of the electron-spin resonance provided information on the temperature dependence of the local susceptibilities, particularly in the important transitional temperature range between 54 and 38 K. In this range, both the electron-spin-resonance and proton relaxation data show that the contribution to the total susceptibility from the TCNQ chains falls more rapidly than that from the TTF chains. However, both techniques involve a weighted average of the individual chain susceptibilities so that the deconvolution requires specific assumptions. Earlier studies of the spin susceptibility[31] and the nuclear relaxation rates[29] have indicated that the observed electronic properties are not dominated by strong Coulomb correlation effects and have provided quantitative information on the energy bandwidth.

Theoretical studies[32] have shown that the Peierls-

Fröhlich state in the 1D fluctuation regime below the mean-field transition temperature $T_\rho^{MF}$ is characterized by a pseudogap in the electronic density of states. In this regime ($T < T_\rho^{MF}$) the magnetic susceptibility is given by

$$\chi = 2\mu_B^2 N(0) . \quad (1)$$

The density of states in the pseudogap is given by

$$N(0) = N_0 \hbar v_F \xi^{-1}(T)/2\Delta , \quad (2)$$

where $N_0$ is the unperturbed band density of states, $v_F$ is the Fermi velocity, $\xi(T)$ is the longitudinal coherence length, and $2\Delta \equiv 2\langle\Delta^2\rangle^{1/2}$ is the energy gap ($2\Delta = 3.5\, k_B T_\rho^{MF}$). Thus the temperature dependence of the susceptibility can provide direct information on the temperature dependence of the coherence length.

In this paper we present a study of the Knight shift and nuclear spin-lattice relaxation time ($T_1$) associated with the $^{13}$C labeled CN group located on the TCNQ molecule in TTF-TCNQ. The Knight shift in metals is given by[33]

$$K = \Delta H/H_0 = -\mu_B^{-1} H_{hf} \chi_i , \quad (3)$$

where $\Delta H$ is the shift in resonance field ($H_0$) due to the conduction electrons, $H_{hf}$ is the average hyperfine field per electron, and $\chi_i$ is the Pauli (local) susceptibility per molecule. The Knight shift thus provides a direct measure of the time-averaged local magnetic field at the TCNQ molecule and thereby determines the temperature dependence of the TCNQ chain local magnetic susceptibility. When combined with the previously published total susceptibility, $\chi_T$, the data can be analyzed to obtain the individual chain contributions ($\chi_Q$ for the TCNQ chains and $\chi_F$ for the TTF chains). The experimental results are presented in Sec. II. The data are discussed in Sec. III and analyzed together with the total spin susceptibility to obtain the local contributions, $\chi_Q$ and $\chi_F$. In Sec. IV, the temperature-dependent coherence length is calculated using the Ginzberg-Landau theory for the case of a complex order parameter.[34] The implied susceptibility [Eqs. (1) and (2)] is in good agreement with the experimentally determined $\chi_Q(T)$. In addition, the pinning transition is discussed in the context of the temperature-dependent coherence length. The $^{13}$C nuclear relaxation data are discussed in Sec. V in a further attempt to determine the relative strength of the effective Coulomb interaction. Section VI presents a brief summary and discussion of the local susceptibility results in the context of recent theoretical ideas concerning the phase transitions in TTF-TCNQ.

## II. EXPERIMENTAL

The $^{13}$C NMR observations were performed on a sample of TTF-TCNQ in which the cyanide (CN) carbon atoms of the TCNQ molecule were selectively enriched to a level of 50%; the natural abundance of $^{13}$C is only 1%. Figure 1(a) shows the molecular structures of TTF and TCNQ indicating the $^{13}$C labeled CN groups. Wideline measurements were made with a Varian WL-112 NMR spectrometer operating at frequencies from 6 to 21 MHz. Temperatures from 4.2 to 300 K were maintained by cold gas-flow systems and measured with a calibrated Ge resistance thermometer.

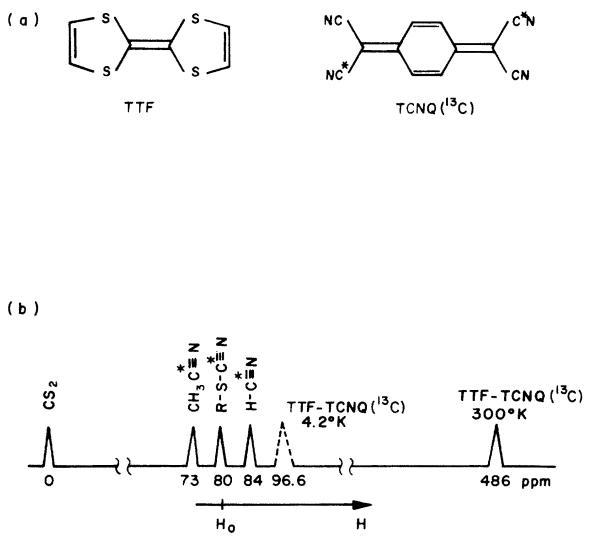


FIG. 1. (a) TTF and TCNQ molecules. $^{13}$C enriched CN carbon positions on the TCNQ molecule are randomly *cis-trans*. (b) Range of the $^{13}$C NMR shift $\delta$ in TTF-TCNQ ($^{13}$C) is illustrated at 4.2 and 300 K relative to $CS_2$. Chemical shifts of other CN carbon compounds are shown for comparison.

The $^{13}$C wideline NMR spectrum is nearly symmetric with a width (defined as the splitting between derivative maxima) of 3.8–4.0 G. This width is independent of applied magnetic field strength and temperature. Room-temperature second-moment measurements of the resonance line at 10, 15, and 21 MHz yield a field-independent value of $2.6 \pm 0.3$ G, consistent with known dipolar coupling strengths in the system.

Shifts were measured with respect to natural $^{13}$C in methanol. The shift decreases monotonically as the temperature is lowered from $+340 \pm 10$ ppm at 298 K to $-48$ ppm at 4.2 K (the positive sign here indicates an upfield shift). The errors in these shift determinations are not uniform. For $T < 45$ K and $T > 135$ K, sensitivity problems limit the accuracy of the shift determination from a single measurement to $\pm(20–30)$ ppm. For $45 < T < 135$ K, the relatively strong signal permits shift determinations of $\pm(5–10)$ ppm. In addition to these relative uncertainties, an absolute error estimated at $\pm 10$ ppm is associated with second-

ary effects such as diamagnetic polarization of the standard. Below 45 K, the resonance line is easily saturated, indicating a dramatic increase in $T_1$ below the transition region.

The significance of these shift magnitudes is shown in Fig. 1(b). Methanol has a shift of +145 ppm upfield from the $CS_2$ standard customarily chosen as the zero of the $^{13}C$ chemical shift scale.[35] In terms of the $CS_2$ standard, the $^{13}C$ shift in TTF-TCNQ varies from +486 ppm at 298 K to 97 ppm at 4.2 K. The observed shift at 298 K is far outside the range of normal chemical shifts and thus is associated with an unpaired electron density on the TCNQ molecule. By contrast, the 4.2 K value is very similar to the $^{13}C$ shifts observed for a broad class of $^{13}CN$ configurations[35] (73 ppm–84 ppm) shown in Fig. 1(b). The close proximity to the neutral molecular values at 4.2 K suggests there is no unpaired electron density and hence no magnetism on the TCNQ molecules at low temperatures. The full temperature dependence of the $^{13}C$ shift measured at 15 MHz is shown in Fig. 2.

The $^{13}C$ relaxation time, $T_1$, was measured directly at 10 MHz with a pulse spectrometer using the 90° saturating comb-$\tau$-90° pulse technique. A boxcar signal averager was used to monitor the magnetization after the final (signal) pulse. A semilog plot of magnetization versus time delay ($\tau$) was consistent with the assumption of a single relaxation time. Temperatures from 4.2 to 300 K were obtained by a cold gas flow balanced by a feedback controlled heater. A temperature stability of ±0.1 K was maintained over the period of the measurement. All temperature measurements were made with a calibrated copper resistance thermometer. The $T_1$ data are shown in Fig. 3. The rate decreases in a fashion similar to that found for protons. At low temperatures (below 50 K) the relaxation time could not be accurately measured because the hold time of the boxcar signal averager was exceeded. The long relaxation time at low temperatures is in agreement with the qualitative observation of easy saturation of the line in the continuous-wave NMR studies.

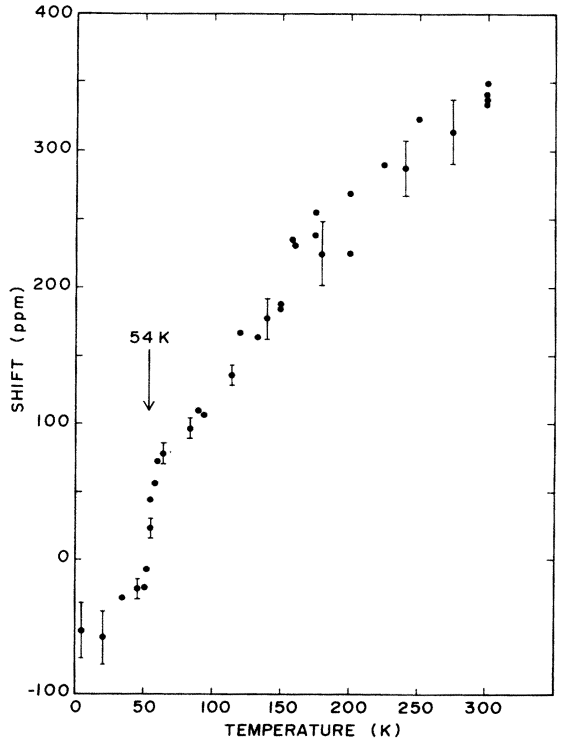


FIG. 2. $^{13}C$ Knight shift (in ppm) as a function of temperature. Representative error bars in the various temperature ranges are shown.

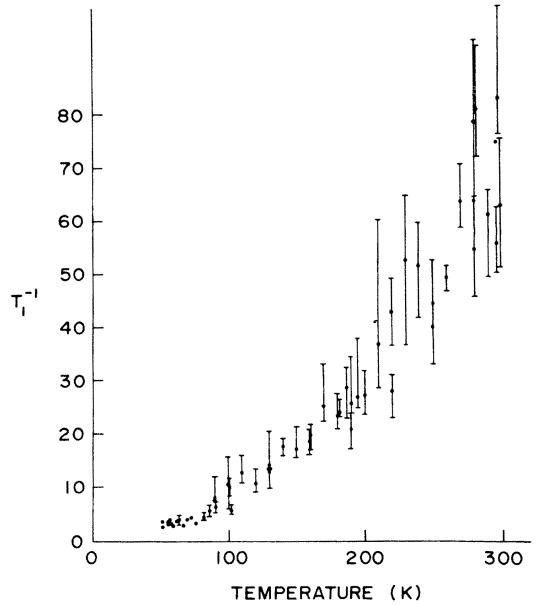


FIG. 3. $^{13}C$ spin-lattice relaxation rate $T_1^{-1}$ vs temperature.

## III. DISCUSSION AND ANALYSIS OF EXPERIMENTAL RESULTS

A plot of the Knight shift versus the total static susceptibility $\chi_T = \chi_Q + \chi_F$ (the sum of the individual chain susceptibilities) is shown in Fig. 4. If the local susceptibility on the TCNQ molecule $\chi_Q(T)$ had the same temperature dependence as the total susceptibility $\chi_T$, then the $K(T)$ vs $\chi_T(T)$ plot should be linear for the case of a constant hyperfine field. The fact that $K(T)$ (and hence $\chi_Q$) is not linearly related to $\chi_T$ implies that the TCNQ susceptibility

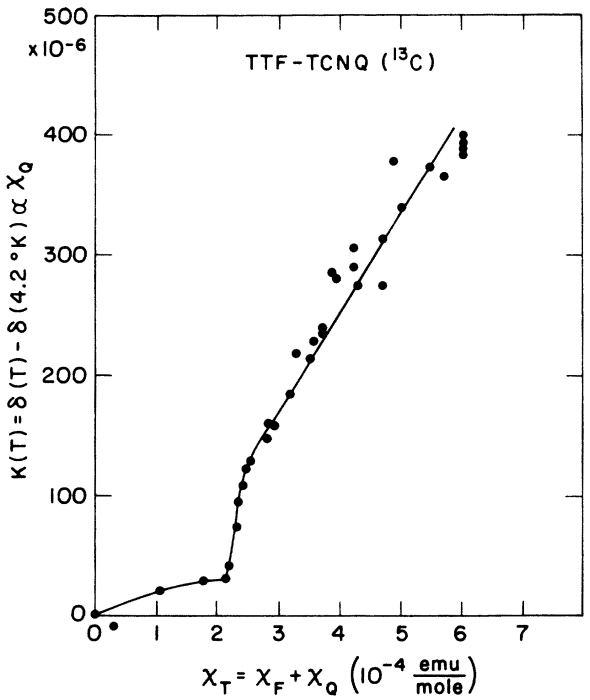


FIG. 4. $^{13}$C Knight shift, $K(T)$, vs total static susceptibility $\chi_T(T)$. Temperature is an implicit parameter.

has a temperature dependence which is different from the total susceptibility. Hence Fig. 4 is a direct indication that the two chains have a different character and gives support for an independent two-chain model description of TTF-TCNQ.

Above 80 K, the Knight shift varies approximately linearly with the susceptibility on the TCNQ chain;

$$\chi_T = A\chi_Q + B\,, \tag{4}$$

where $A$ and $B$ are constants ($B \simeq 0.9\times10^{-4}$ emu/mole). Since $\chi_T = \chi_F + \chi_Q$, Eq. (4) implies that in this high-temperature regime

$$\chi_F = (A-1)\chi_Q + B\,. \tag{5}$$

A change of slope occurs near 54 K as a result of the onset of order on the TCNQ chain. Below 54 K, the Knight shift (or susceptibility) on the TCNQ chain is essentially zero [< 8% of K (300 K)], whereas the total static susceptibility has decreased only to $\frac{1}{3}$ of its room-temperature value $\chi_T$(300 K). We conclude that the TCNQ chain susceptibility is almost zero below 54 K, and the remaining susceptibility is due to the TTF chain. The residual susceptibility on the TCNQ chain below 54 K is apparently due to single-particle excitations across the energy gap. The sensitivity of the Knight-shift measurement is insufficient to determine the detailed temperature dependence in the low-temperature regime below 54 K. However, Tomkiewicz, Taranko, and Torrance[30] have used the $g$-value analysis in this region of temperature to infer $2\Delta \simeq 880$ K in relatively good agreement with the earlier results obtained directly from infrared studies.

Using the Knight-shift data, we will decompose the total susceptibility into the individual TTF and TCNQ chain susceptibilities. The TTF susceptibility is simply

$$\chi_F = \chi_T - \chi_Q \text{ or } \chi_F(T) = \chi_T(T) - \alpha K(T)\,,$$

where $K(T)$ is the $^{13}$C Knight shift on the TCNQ chain and $\alpha$ is the normalization constant defined by Eq. (3) ($\alpha = \mu_B H_{\rm hf}^{-1}$). The absolute values of $\chi_Q(T)$ and $\chi_F(T)$ can be determined from the Knight shift together with the total susceptibility by determining the ratio $\chi_Q/\chi_F$ at any fixed temperature. This ratio can be estimated from the proton spin-lattice relaxation rates $T_1^{-1}$. In metals, the relaxation rate is given by the Korringa relation,[33,36]

$$\chi^2 T_1 T = \hbar\mu_B^2/\pi k_B a_{\rm H}^2 \mathcal{K}(\mu, T)\,. \tag{6}$$

This relation has been shown to describe the observed behavior of TTF-TCNQ above 54 K. The proton hyperfine constant $a_{\rm H}$ can be estimated from solution studies [$a_{\rm H}$(TCNQ) = 1.57 G; $a_{\rm H}$(TTF) = 1.26 G].[37] If the Coulomb enhancement factors $\mathcal{K}(\mu, T)$ are assumed to be of order unity and equal on both chains, then the ratio of the individual chain susceptibilities is proportional to the ratio of the square root of the corresponding relaxation rates.

$$\frac{\chi_Q\ (300\ \text{K})}{\chi_F\ (300\ \text{K})} = \frac{a_{\rm H}^F}{a_{\rm H}^Q}\left(\frac{T_1^F}{T_1^Q}\right)^{1/2}\,. \tag{7}$$

Using $\chi_F + \chi_Q = \chi_T$, we find

$$\frac{\chi_F}{\chi_T} = \left[1 + \frac{a^F}{a^Q}\left(\frac{T_1^F}{T_1^Q}\right)^{1/2}\right]^{-1}\,. \tag{8}$$

Hence at 300 K; $\chi_F/\chi_T \simeq 0.66$; $\chi_Q/\chi_T \simeq 0.34$. The decomposed individual chain susceptibilities are shown in Figs. 5(a)–5(c) for assumed values of $\chi_Q/\chi_T = 0.3$, 0.34, and 0.4 at room temperature, respectively. Figure 5(a) represents our best estimate of the individual chain susceptibilities. Values for $\chi_Q$(300 K)/$\chi_T$(300 K) greater than 0.3 lead to nonmonotone behavior for $\chi_F$ in the vicinity of 50 K; a result which we find unacceptable in view of the earlier $T_1$ data[29] which show $(T_1T)^{-1/2}$ for the TTF chain to be monotonic with a flat plateau near 50 K in agreement with Fig. 5(a).

The temperature-dependent local susceptibilities as obtained directly from analysis of the $^{13}$C Knight shift data are quite different from the decomposition of $\chi_T$ assumed by Scott, Garito, and Heeger[31] in their earlier analysis of the bulk susceptibility. Both $\chi_Q$ and $\chi_F$ are temperature de-

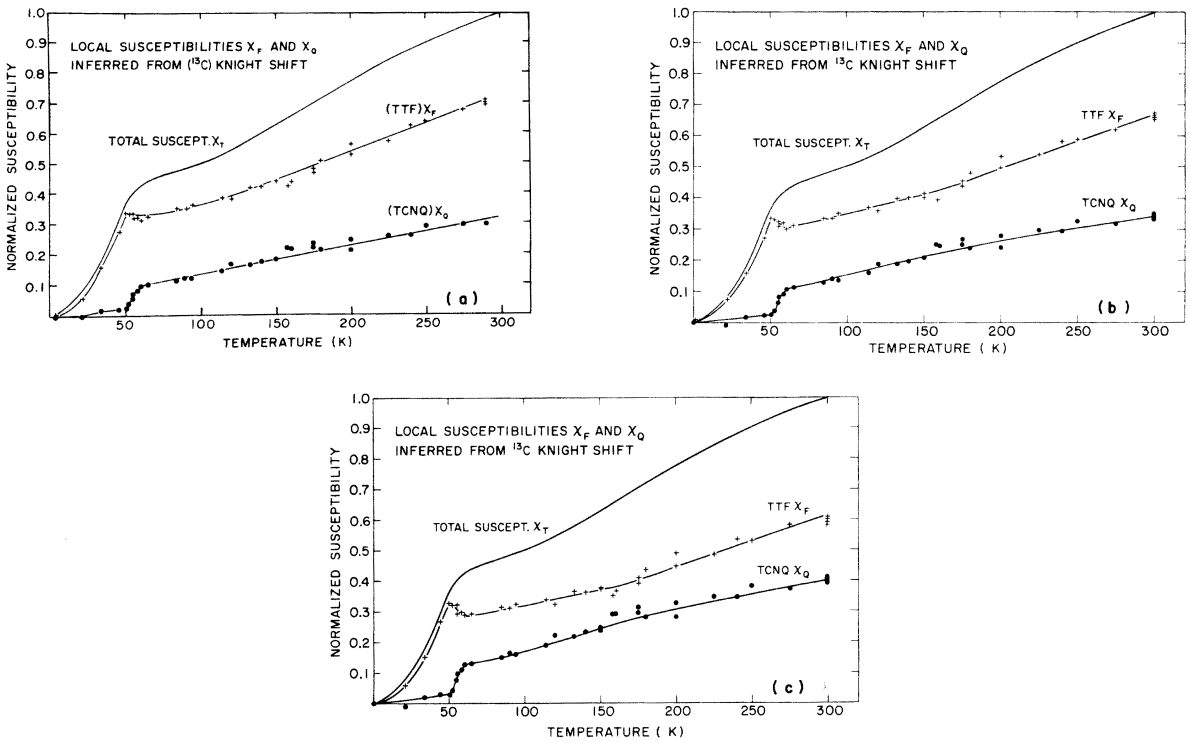


FIG. 5. Normalized local susceptibilities on the TTF ($\chi_F$) and TCNQ ($\chi_Q$) chains with different normalizations of $\chi_Q$ at 300 K (see text). (a) $\chi_Q$ (300 K) = 0.30 $\chi_T$ (300 K). (b) $\chi_Q$ (300 K) = 0.34 $\chi_T$ (300 K). (c) $\chi_Q$ (300 K) = 0.40 $\chi_T$ (300 K).

pendent, and $\chi_F(T) > \chi_Q(T)$ at all temperatures as indicated in Eq. (5) and Fig. 5(a).

An estimate of the electron spin density on the CN site in TCNQ can be obtained from the $^{13}$C Knight shift. In Fig. 4, the constant slope of $K$ vs $\chi_T$ above 80 K indicates that the hyperfine field is temperature independent. Assuming the TCNQ susceptibility at 300 K is approximately $\chi_Q = 0.30\ \chi_T$, then the value of the hyperfine field $H_{hf}$ [from Eq. (3)] is 12 kG [$A/g\mu_B = 9$ G; $A/g\mu_B = 2H_{hf}(\gamma_N/\gamma_e)$]. The result compares favorably with the hyperfine coupling constant found for the closely related $\pi$ acceptor, tetracyanoethylene (TCNE), $H_{hf} = 12.4$ kG, $A/g\mu_B = 9.47$ G.[38] The smaller hyperfine field for TCNQ is reasonable since the unpaired electron can delocalize over the larger TCNQ molecule. Assuming 25% of the transferred electron is on each CN group in $(TCNE)^-$, the ratio of the hyperfine fields indicates that 23% of the electrons are on each CN group of the $(TCNQ)^-$ ion.

At room temperature, the $^{13}$C resonance is shifted far upfield [$\delta(300) - \delta(4.2) = 389$ ppm] relative to diamagnetic molecules containing CN groups, indicating that the local magnetic field is opposite to the applied external magnetic field. In the alkali metals, the electron-nuclear coupling occurs directly via the Fermi contact interaction ($A\vec{I}\cdot\vec{S}$) resulting in a downfield shift of the nuclear resonance. Upfield shifts are generally due to core polarization of the inner $s$ electrons by the outer $p$ or $d$ electrons. The unpaired electron on the TCNQ molecule is in a $\pi^*$ state with a wave function predominantly made up of a linear combination of $2p$ atomic orbitals. Since the unpaired $\pi^*$ electron has no spin density at the $^{13}$C nucleus, the contribution to the total Knight shift from the contact interaction is zero; the Knight shift results from core polarization. Hence the fact that the $^{13}$C resonance is upfield simply reflects the $p$ character of the unpaired electron on the TCNQ molecule.

The individual chain susceptibilities can be used to predict the isotropic average of the ESR $g$-shift tensor. Tomkiewicz *et al.*[30] presented the temperature dependence of the ESR $g$ shifts and analyzed their results in terms of the average of the individual molecular $g$ shifts, weighted by the local molecular susceptibilities

$$g = g_Q\chi_Q/\chi_T + g_F\chi_F/\chi_T, \tag{9}$$

where $g_{Q,F}$ are the solution $g$ shifts found for TCNQ (2.0025) and TTF (2.00 838) molecules, and $\chi_{Q,F}$ are the local susceptibilities. Substituting the local susceptibility as obtained from Fig. 5(a), the calculated temperature-dependent $g$ shift using Eq. (9) is shown in Fig. 6. The experimental $g$-

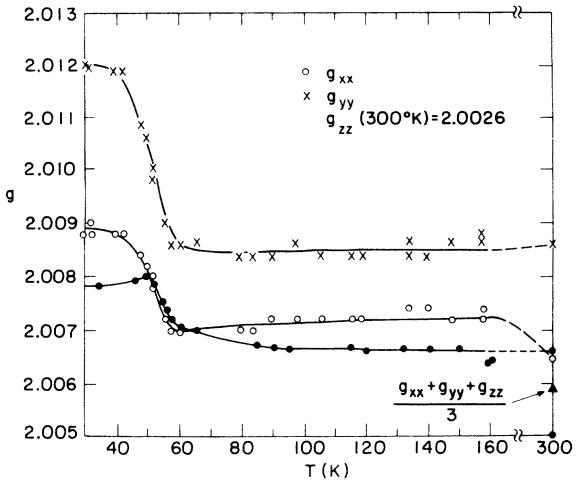


FIG. 6. Comparison of the experimental electron spin resonance $g$ value (○○○ and ××× from Ref. 30) with the isotropic average (●●●) inferred from the local susceptibilities through Eq. (9).

tensor data of Tomkiewicz *et al.*[30] are also plotted. The temperature dependence of $g_{zz}$ was not reported. The NMR result is a measure of the isotropic average of the $g$ tensor, $\frac{1}{3}[g_{xx}(T)+g_{yy}(T)+g_{zz}(T)]$. The overall agreement shown in Fig. 6 is relatively good; the coarse features of the temperature dependence of the $g$ shift are reproduced by the NMR-determined local susceptibilities. Since the electron interchain hopping time is much shorter than either the NMR or ESR precession periods, the small deviations in absolute magnitude possibly result from the oversimplified analysis based on Eq. (9). A more realistic approach would take into account a Fermi-surface average of the $\vec{k}$-dependent metallic $g$ tensor. The increase in $g$ at low temperatures occurs because the TCNQ susceptibility goes to zero, and hence the $g$-value shifts from an average value to a higher value are characteristic of the TTF monoradical cation.

## IV. TEMPERATURE-DEPENDENT COHERENCE LENGTH

The $^{13}$C Knight-shift results indicate that at approximately 54 K a real energy gap opens in the electronic excitation spectrum of the TCNQ chains, and the susceptibility drops rapidly to zero. At higher temperatures in the 1D fluctuation regime, theoretical studies[32] have proposed that the density of states and the corresponding susceptibility are determined by the coherence length for the fluctuating charge-density wave as described by Eqs. (1) and (2). Within the model the gap is relatively well formed with $\xi(T) \gg b$ so that the density of states is smaller than the simple band-structure value and the fluctuating charge-density wave slides via time-dependent phases to contribute to the dc conductivity. Infrared experiments on polycrystalline[10] and single-crystal[11-13] samples have confirmed the existence of the pseudogap at temperatures above 54 K. However, the infrared conductivity studies do not yield direct information on the density of states for $\hbar\omega < 2\Delta$ since the mobility may be limited by strong scattering of the electrons by fluctuations associated with the dynamic Peierls distortion.

The interpretation of the dc conductivity as resulting from collective-mode motion implies that the order parameter should be complex with amplitude and phase as independent parameters. The coherence length for the complex order-parameter case can be calculated using the theory of Scalapino, Sears, and Ferrell.[34] These authors treat the complex Ginzburg-Landau field starting with the free-energy functional

$$F = \int dx(a|\Psi|^2 + b|\Psi|^4 + c|d\Psi/dx|^2) .$$

where $\Psi = \Psi_0 e^{i\varphi}$ is the complex order parameter, and $a$, $b$, and $c$ are phenomenological constants to be obtained from microscopic theory for application to a particular problem. The statistical mechanics is solved by transformation to an equivalent one-particle (anharmonic oscillator) quantum-mechanics problem with Hamiltonian[34] $H = -(4\beta^2 c)^{-1} d^2/d\Psi^2 + a|\Psi|^2 + b|\Psi|^4$, where $\beta = (k_B T)^{-1}$. With this transformation,[34]

$$\xi(T)^{-1} = \beta(E_1 - E_0) , \tag{10}$$

where $E_0$ and $E_1$ are the ground-state and first-excited-state energies of the Hamiltonian.

We consider the case $T \ll T_p^{\mathrm{MF}}$, where $T_p^{\mathrm{MF}}$ is the mean-field Peierls temperature defined by

$$3.5 k_B T_p^{\mathrm{MF}} = 2\Delta = 2|\Psi_0(0)| , \tag{11}$$

where $\Psi_0(0) = \langle \Psi_0(T=0) \rangle$ and $2\Delta = E_g$ is the energy gap. For this temperature regime, the free energy has formed a distinct minimum for $|\Psi| \neq 0$ but with arbitrary phase; the Fröhlich state.[16] Since amplitude fluctuations are more energetically costly, the continuous phase-only case will be considered for $\Psi$ complex, $\Psi = |\Psi_0(0)| e^{i\varphi}$, and only phase fluctuations are included. The Hamiltonian then takes the particularly simple form of a rigid rotor,

$$H = -[4\beta^2 c|\Psi_0(0)|^2]^{-1} d^2/d\varphi^2$$

and

$$E_i = (4\beta^2 c)^{-1}[|\Psi_0^2(0)|]^{-1} m^2 , \tag{12}$$

where $m = 0, 1, \ldots$ . We have initially neglected possible $\varphi$-dependent pinning potentials (e.g., impurities, commensurability, interchain Coulomb coupling, etc.) which would tend to fix $\varphi$.

The coherence length is therefore given by [Eq. (10)]:

$$\xi(T)^{-1} = k_B T/4c|\Psi_0(0)^2| \,. \tag{13}$$

The quantity $c|\Psi_0^2(0)|$ can be obtained from microscopic theory. Rice *et al.*[39] have shown that to obtain the linear phase phonons[32] the potential energy for compression of the charge-density wave should be of the form

$$E^{p}_{\text{compression}} = \frac{m v_F^2 N_s}{2} (2k_F)^{-2} \left|\frac{d\varphi}{dx}\right|^2 .$$

Therefore,

$$c\left|\frac{d\Psi}{dx}\right|^2 = c|\Psi_0^2(0)|\left|\frac{d\varphi}{dx}\right|^2$$

$$= \frac{m v_F^2}{2} N_s (2k_F)^{-2} \left|\frac{d\varphi}{dx}\right|^2 . \tag{14}$$

$N_s = N_e/L = f/b$ is the condensate density and $f$ is the fractional charge transfer.

$$4c|\Psi_0(0)|^2 = (\tfrac{1}{2} m v_F^2)(f/b) k_F^{-2} \tag{15}$$

and

$$\xi_{(T)}^{-1} = (kT/\tfrac{1}{2} m v_F^2) k_F^2 (b/f) \,. \tag{16}$$

Finally, using Eqs. (1) and (2):

$$\chi_{(T)} = \frac{\pi}{2} \frac{kT}{\Delta} \chi_p \simeq \chi_p \frac{T}{T_p^{\text{MF}}} \,, \tag{17}$$

where $\chi_p = 2\mu_B^2 N_0$ is the bare Pauli susceptibility.

The TCNQ chain susceptibility, $\chi_Q(T)$, from Fig. 5(a) is replotted in Fig. 7 along with the theoretical curve from Eq. (17) assuming $T_p^{\text{MF}} \simeq 300$ K ($3.5\ k_B T_p^{\text{MF}} \simeq 0.1$ eV) (Refs. 10–13) and $\chi_p \simeq 2\mu_B^2/W$ with a bandwidth $W \simeq 0.35$ eV in agreement with earlier experimental[1,8,13,40] and calculated[41] results. The measured susceptibility increases approximately linearly with increasing temperatures with a magnitude in good agreement with theory. As $T \to T_p^{\text{MF}}$, amplitude fluctuations are expected to become important so that $\xi(T)$ would decrease more rapidly than $T^{-1}$. The observed linearity of $\chi(T)$ all the way to room temperature may result from a partial cancellation of the small increase due to amplitude fluctuations balanced by the decrease arising from the temperature dependence of the narrow-band Pauli susceptibility. We conclude that the density of states as measured by the local susceptibility is consistent with the complex order-parameter description in the 1D fluctuation regime above 54 K. Below 54 K, the charge-density wave (CDW) becomes pinned giving the large low-frequency dielectric constant. The coherence length grows rapidly in the pinned regime causing the susceptibility to decrease dramatically, as observed.

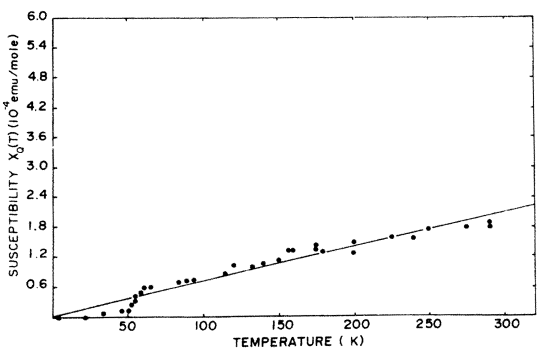


FIG. 7. TCNQ chain susceptibility, $\chi_Q$, vs temperature. Data points were obtained directly from $^{13}$C Knight-shift analysis; solid line is Eq. (17).

The discussion of the previous paragraphs ignores the existence of a phase-dependent potential which at low enough temperatures will pin the CDW. Although we will explicitly treat the case where interchain Coulomb coupling is the dominant phase-locking mechanism, the results discussed below are at least qualitatively valid for high-order commensurability pinning as well. The simplest form for the phase-dependent potential is given by

$$V(\varphi) = V_0(1 - \cos\varphi) \,, \tag{18}$$

where $\varphi$ is the CDW phase relative to that of the nearest-neighbor chains which are assumed to be ordered (a mean-field theory). The phase is pinned by the potential when the coherence length is sufficiently long that the energy for a fluctuation exceeds $k_B T$. Thus[42,43]

$$eV_0 N_s \xi(T_{\text{pin}}) \simeq k_B T_{\text{pin}} \tag{19}$$

is the pinning condition. For $T < T_{\text{pin}}$, the CDW is fixed in space and restricted to small oscillations at a frequency determined by

$$V(\varphi) \simeq \tfrac{1}{2} V_0 \varphi^2 \,, \tag{20}$$

$$V(x) \simeq \tfrac{1}{2} V_0 (2k_F)^2 x^2 \,. \tag{21}$$

The CDW equation of motion is therefore

$$M^* \ddot{x} + eV_0(2k_F)^2 x = 0 \,, \tag{22}$$

where $M^*$ is the Fröhlich effective mass. The experimentally determined pinning frequency, $\omega_F$, therefore can be used to obtain the magnitude of $V(\varphi)$;

$$\omega_F^2 = (eV_0/M^*)(2k_F)^2 \,. \tag{23}$$

Combining Eqs. (16), (19), and (23), we obtain the pinning temperature

$$k_B T_{\text{pin}} \simeq (1/\pi k_F)(M^* \omega_F^2 E_F)^{1/2} \,. \tag{24}$$

Values for $M^*$ and $\omega_F$ have been obtained from

far-infrared reflectance studies,[12] $M^* \simeq 1500\, m$ where $m$ is the band mass and $\omega_F \simeq 2$ cm$^{-1}$; $\lambda_s f = 2b$,[18,19] and $E_F \simeq 0.1$ eV as discussed above. Using these values in Eq. (24) yields $T_{\text{pin}} \simeq 40$ K in quite reasonable agreement with the observed value. Moreover, the magnitude of $V_0$ is consistent with rough estimates based on Coulomb interchain coupling.[44] At the pinning temperature, the longitudinal coherence length as calculated from Eq. (16) is approximately 60 lattice constants in agreement with estimates obtained from the diffuse x-ray[18] and elastic neutron scattering[20] results. Taking into account the expected temperature dependence due to the combined phase [Eq. (16)] and amplitude fluctuations, the coherence length at room temperature should be only a few lattice constants (approximately five).

## V. $^{13}$C NUCLEAR RELAXATION STUDIES AND ROLE OF THE COULOMB INTERACTION

The relative importance of the repulsive Coulomb interaction in TTF-TCNQ has been the subject of considerable discussion. In general, one expects that Coulomb correlations might play a dominant role in such narrow-band systems. This has been shown to be the case through experimental studies of N-methylphenazinium-tetracyanoquinodimethane (NMP)(TCNQ),[36,45] and potassium-tetracyanoquinodimethane K(TCNQ).[46] However, for TTF-TCNQ the available experimental evidence[29,31] indicates that for frequencies well below the plasma frequency,[8,9] the Coulomb interaction is screened by the full dielectric response of the medium[47] and the effective interaction is relatively weak, and possibly attractive. The absence of local moment formation, the nonmagnetic ground state,[31] and the simple Korringa relaxation for the protons[29] all indicate a weak repulsive electron-electron interaction for TTF-TCNQ. The $^{13}$C relaxation rates presented in this paper provide additional support of this conclusion.

The $^{13}$C relaxation rate is shown as a function of temperature in Fig. 3. The data are replotted in Fig. 8 as $(K^2T_1T)$ vs $T$ where $K$ is the Knight shift obtained directly from experiment.

For an isotropic simple metal, where the Fermi contact interaction is the sole electron-nuclear coupling, the Korringa relation yields[33]

$$K^2T_1T = (\hbar/4\pi k_B)(\gamma_e/\gamma_N)^2 . \tag{25}$$

The effect of nonisotropic contributions[48] (e.g., electron-nuclear dipolar) is to leave the temperature dependence unchanged but to decrease the magnitude of $(K^2T_1T)$ since the Knight shift results from only the isotropic part of the interaction whereas the full interaction contributes to $T_1^{-1}$. An additional temperature-dependent enhancement

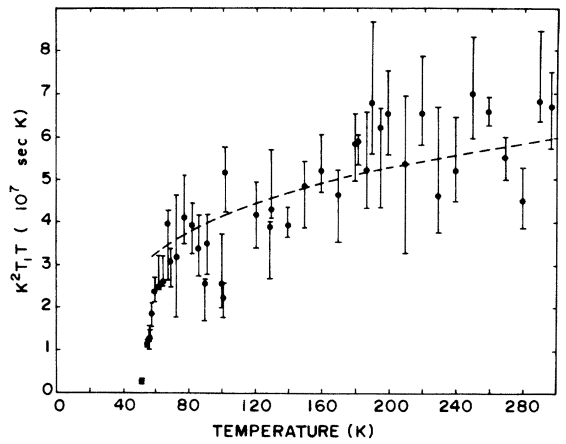


FIG. 8. $K^2(T)\,T_1T$ vs temperature for $^{13}$C in TTF-TCNQ ($^{13}$C). Dashed line is the temperature dependence calculated from Eq. (26) using $\mu = UN_0 = 0.15$ (see text).

factor is expected from the Coulomb interaction in a quasi-one-dimensional metal.[36] Treating the Coulomb effects in the random-phase approximation, one obtains

$$K^2T_1T = D\mathcal{K}(\mu, T)(K^2T_1T)_0 , \tag{26}$$

where $(K^2T_1T)_0$ is given by Eq. (25), $D$ is the temperature-independent anisotropy coefficient, and

$$\mathcal{K}(\mu, T) \cong \langle[1 - \mu F(2k_FT)]^2\rangle \tag{27}$$

is the temperature-dependent enhancement factor which is determined by the strength of the electron-electron Coulomb interaction $U$, $\mu = UN_0$, and $N_0$ is the density of states. In a one-dimensional electronic system such as TTF-TCNQ, the Lindhard response function $F(q, T)$ peaks at $q = 2k_F$ and is strongly temperature dependent. As a result $T_1^{-1}$ measurements are particularly sensitive to Coulomb interactions.[36] The inclusion of the coupling of the electrons to acoustic phonons, intramolecular phonons, and excitons leads to an effective total interaction, $\mu_{\text{eff}}$, which can be small, or even attractive ($\mu_{\text{eff}} < 0$). Although the random-phase approximation treatment breaks down in a 1D system because of the instability, Eqs. (26) and (27) express at least qualitatively the effect of interactions on the relaxation rate.

The data of Figs. 4 and 8 can be compared with Eqs. (26) and (27). Although $T_1^{-1}$ decreases by more than an order of magnitude from 300 to 60 K, $K^2T_1T$ is approximately constant decreasing slowly with decreasing temperature. This result is consistent with the earlier $T_1$ measurements on protons[29] in TTF-TCNQ, which indicated a Coulomb enhancement factor of order unity. The slow decrease of $K^2T_1T$ may be due to residual repulsive interactions. The dashed curve on Fig. 8 is a plot of Eq. (26) using $\mu = UN_0 = 0.15$ and $E_F = 0.1$

eV with $F(2k_F, T) \sim \ln(E_F/kT)$. This may be considered an upper limit for $\mu$ since larger values would yield too strong a temperature dependence. Using $N_0 = (2\sqrt{2}/\pi)W^{-1} \simeq W^{-1}$ as the density of states for the approximately quarter-filled band of width $W \simeq 0.3$–$0.4$ eV,[1,8,13,40,41] the enhanced Korringa analysis yields the magnitude of the on-site Coulomb interaction, $U < 0.1$ eV. Additional relaxation may be expected when the coherence length grows long so that the associated fluctuations in the density of states slow down to frequencies comparable with the NMR frequency. Such effects may play a role in the sharp decrease of $K^2T_1T$ observed below 60 K.

The asymptotic value of $K^2T_1T$ at high temperatures is approximately a factor of 5 smaller than that given by the isotropic Korringa relation [Eq. (25)]. As suggested above, this nearly temperature-independent factor arises at least in part from the anisotropic hyperfine coupling expected for the $^{13}C$ nucleus in the CN group of TCNQ.

## VI. DISCUSSION

Two transformations, at 54 and 38 K, in TTF-TCNQ have been widely studied[2-4,24-26,49-52] with direct structural evidence coming from x-ray[18,19] and neutron studies.[20] Principally by analyzing transport measurements, Etemad[26] suggested that the 54 K transformation results from ordering on TCNQ chains and the 38 K transformation, on TTF chains. From elastic neutron studies, Comès *et al.*[20] showed that the region $38 < T < 54$ K is characterized by an incommensurate superlattice where the $a$-axis modulation changes continuously from $2a$ near 54 K to $4a$ with a discontinuous step at 38 K. On the basis of their Ginzburg-Landau treatment of the two sets of coupled chains, Bak and Emery[24] have shown the neutron results for TTF-TCNQ are consistent with *three* transitions. They suggested long-range order sets in on one of the chains at 54 K and on the second chain near 49 K with the $a$-axis modulation remaining at $2a$ between 54 and 47 K. From 49 to 38 K both chains continuously order with respect to one another, finally locking discontinuously to $4a$ at 38 K. Recently further neutron measurements[25] have provided direct confirmation of the Bak-Emery proposal. The Knight-shift data given in Fig. 9 directly identify the transitions; the TCNQ chains order at 54 K and the TTF chains near 49 K.

The value of the Peierls gap, $2\Delta$, obtained from the $^{13}C$ Knight-shift studies above 54 K ($2\Delta$ of approximately 0.1 eV) is comparable to that inferred from the temperature dependence of the $g$ value[29] ($2\Delta \simeq 0.08$ eV) below 54 K. Moreover, the infrared results from polycrystalline films[10] and single crystals[11-13] both above and below 54 K indicate a value for $2\Delta$ of the same magnitude. We therefore conclude that in agreement with earlier analysis,[10-13,31,32] the mean-field Peierls temperature for the TCNQ chains is of order 400 K and that the entire temperature range from 300 to 54 K is in the 1D fluctuation regime where $\xi(T)/b \gg 1$.

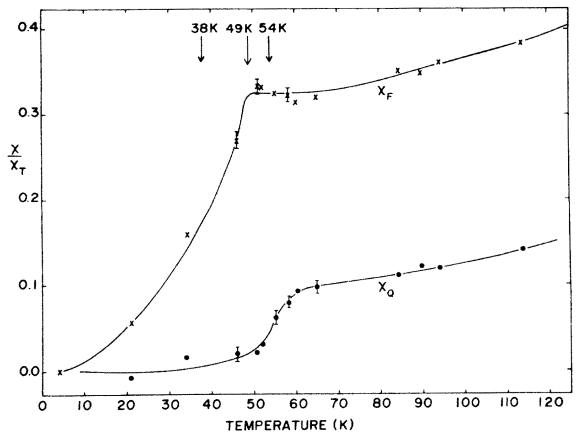


FIG. 9. Temperature dependence of the TTF and TCNQ chain local susceptibilities shown in detail in the transition region.

The complete temperature dependence of $\chi_Q(T)$ may be represented quantitatively by the Peierls-Fröhlich model with a *complex* order parameter describing the broken symmetry state for $T > 54$ K [Eq. (17)] which becomes pinned when the phase is essentially locked below 54 K. Systematic studies of the thermoelectric power in TTF-TCNQ,[53] tetraselenafulvalene-tetracyanoquinodimethane (TSeF-TCNQ),[54] and dilute alloys (Ref. 54) $(TTF)_{1-x}(TSeF)_x$ – TCNQ demonstrated that the conductivity in the "metallic" regime is dominated by the TCNQ chain. Thus, the dc transport occurs on the TCNQ chains in the temperature regime where the CDW fluctuations are building up with a relatively long coherence length which in turn arises from the growth of the complex order parameter. The CDW is therefore mobile and contributes to the total conductivity. Given that $\xi(T)/b \gg 1$, the Peierls gap is well formed so that the single-particle contribution to the conductivity should be small, in agreement with the conclusions drawn from the infrared studies.[10-13] Thus the Fröhlich CDW collective mode appears to be the primary transport mechanism in TTF-TCNQ above 54 K.

## ACKNOWLEDGMENTS

We thank Professor D. J. Scalapino for helpful conversations on the temperature dependence of the coherence length, and Paul Nigrey for careful sample preparation.

*Work at the University of Pennsylvania supported by the NSF through Grant No. DMR-74-22923 and through the Laboratory for Research on the Structure of Matter (DMR-72-03025), and by the Advanced Research Projects Agency through Grant No. DAHC-15-72-C-0174.

†Present address: Dept. of Chemistry, Massachusetts Institute of Technology, Cambridge, Mass. 02139.

[1]A. J. Heeger and A. F. Garito, *Low-Dimensional Cooperative Phenomena*, edited by H. J. Keller (Plenum, New York, 1975), p. 89; *Collective Properties of Physical Systems*, edited by B. Lundquist and S. Lundquist (Academic, New York, 1973), p. 129; A. F. Garito and A. J. Heeger, Acc. Chem. Res. 7, 232 (1974).

[2]J. H. Perlstein, J. P. Ferraris, V. V. Walatka, and D. O. Cowan, AIP Conf. Proc. 10, 1494 (1972); J. P. Ferraris, D. O. Cowan, V. V. Walatka, and J. H. Perlstein, J. Am. Chem. Soc. 95, 948 (1973).

[3]L. B. Coleman, M. J. Cohen, D. J. Sandman, F. G. Yamagishi, A. F. Garito, and A. J. Heeger, Solid State Commun. 12, 1125 (1973).

[4]M. J. Cohen, L. B. Coleman, A. F. Garito, and A. J. Heeger, Phys. Rev. B 10, 1298 (1974).

[5]S. K. Khanna, E. Ehrenfreund, A. F. Garito, and A. J. Heeger, Phys. Rev. B 10, 2205 (1974).

[6]S. K. Khanna, A. F. Garito, A. J. Heeger, and R. C. Jaklevic, Solid State Commun. 16, 667 (1975).

[7]M. Cohen, S. K. Khanna, W. J. Gunning, A. F. Garito, and A. J. Heeger, Solid State Commun. 17, 367 (1975).

[8]A. A. Bright, A. F. Garito, and A. J. Heeger, Solid State Commun. 13, 943 (1973); Phys. Rev. B 10, 1328 (1974).

[9]P. M. Grant, R. L. Greene, G. C. Wrighton, and G. Castro, Phys. Rev. Lett. 31, 1311 (1973).

[10]D. B. Tanner, C. S. Jacobsen, A. F. Garito, and A. J. Heeger, Phys. Rev. Lett. 32, 1301 (1974).

[11]C. S. Jacobsen, D. B. Tanner, A. F. Garito, and A. J. Heeger, Phys. Rev. Lett. 33, 1559 (1974).

[12]L. B. Coleman, C. R. Fincher, Jr., A. F. Garito, and A. J. Heeger, Phys. Status Solidi B 75, 239 (1976).

[13]D. B. Tanner, C. S. Jacobsen, A. F. Garito and A. J. Heeger, Phys. Rev. B 13, 3381 (1976).

[14]J. Bardeen, Solid State Commun. 13, 357 (1973); D. Allender, J. W. Bray, and J. Bardeen, Phys. Rev. B 9, 119 (1974).

[15]R. E. Peierls, *Quantum Theory of Solids* (Clarendon, Oxford, 1955), p. 108.

[16]H. Frohlich, Proc. R. Soc. A 223, 296 (1954).

[17]A. M. Afanas'ev and Yu. Kagan, Zh. Eksp. Teor. Fiz. 43, 1456 (1963) [Sov. Phys.-JETP 16, 1030 (1963)].

[18]F. Denoyer, R. Comès, A. F. Garito, and A. J. Heeger, Phys. Rev. Lett. 35, 445 (1975).

[19]S. Kagoshima, H. Anzai, K. Kajimura, and T. Ishigoro, J. Phys. Soc. Jpn. 39, 1143 (1975).

[20]R. Comès, S. M. Shapiro, G. Shirane, A. F. Garito, and A. J. Heeger, Phys. Rev. Lett. 35, 1518 (1975); Phys. Rev. B (to be published).

[21]H. A. Mook and C. R. Watson, Phys. Rev. Lett. 36, 801 (1976).

[22]G. Shirane, S. M. Shapiro, R. Comès, A. F. Garito, and A. J. Heeger, Phys. Rev. B (to be published).

[23]T. J. Kistenmacher, T. E. Phillips, and D. O. Cowan, Acta. Crystallogr. B 30, 763 (1974).

[24]Per Bak and V. J. Emery, Phys. Rev. Lett. 36, 978 (1976).

[25]W. D. Ellenson, R. Comès, S. M. Shapiro, G. Shirane, A. F. Garito and A. J. Heeger (unpublished).

[26]S. Etemad, Phys. Rev. B 13, 2255 (1976); S. Etemad, T. Penney, and E. M. Engler, Bull. Am. Phys. Soc. 20, 491 (1975).

[27]M. Barmatz, L. R. Testardi, A. F. Garito, and A. J. Heeger, Solid State Commun. 15, 1299 (1974).

[28]M. J. Rice, C. B. Duke, and N. O. Lipari, Solid State Commun. 17, 1089 (1975).

[29]E. F. Rybaczewski, A. F. Garito, A. J. Heeger, and E. Ehrenfreund, Phys. Rev. Lett. 34, 524 (1975).

[30]Y. Tomkiewicz, B. A. Scott, L. J. Tao, and R. S. Title, Phys. Rev. Lett. 32, 1363 (1974); Y. Tomkiewicz, A. R. Taranko, and J. B. Torrance, Phys. Rev. Lett. 36, 751 (1976).

[31]J. C. Scott, A. F. Garito, and A. J. Heeger, Phys. Rev. B 10, 3131 (1974).

[32]P. A. Lee, T. M. Rice, and P. W. Anderson, Phys. Rev. Lett. 31, 462 (1973); Solid State Commun. 14, 703 (1974). These results have been obtained independently by M. J. Rice and S. Strässler, Solid State Commun. 13, 1389 (1973) and A. Bjeliš and S. Barišić, J. Phys. Lett. (Paris) 36, L169 (1975).

[33]C. P. Slichter, *Principles of Magnetic Resonance* (Harper and Row, New York, 1963).

[34]D. J. Scalapino, M. Sears and R. A. Ferrell, Phys. Rev. B6, 3409 (1972); G. Toulouse, Nuovo Cimento B 23, 234 (1974); R. Balian and G. Toulouse, Ann. Phys. 83, 28 (1974); P. Manneville, J. Phys. (Paris) 36, 70 (1975).

[35]J. A. Pople, W. G. Schneider, and H. J. Bernstein, *High-Resolution Nuclear Magnetic Resonance* (McGraw-Hill, New York, 1959), pp. 306–308.

[36]E. Ehrenfreund, E. F. Rybaczewski, A. F. Garito, and A. J. Heeger, Phys. Rev. Lett. 28, 873 (1972).

[37]P. N. Reiger and G. K. Fraenkel, J. Chem. Phys. 37, 2795 (1962); F. Wudl, G. M. Smith, and E. J. Hufnagel, Chem. Commun. 21, 1453 (1970).

[38]A. Carrington and D. McLachlan, *Introduction to Magnetic Resonance* (Harper and Row, New York, 1967), p. 94.

[39]M. J. Rice, A. R. Bishop, J. A. Krumhansl, and S. E. Trullinger, Phys. Rev. Lett. 36, 432 (1976).

[40]J. J. Ritsko, D. J. Sandman, A. J. Epstein, P. C. Gibbons, S. E. Schnatterly, and J. Fields, Phys. Rev. Lett. 34, 1330 (1975).

[41]A. Karpfen, J. Ladik, G. Stollhoff, and P. Fulde, Chem. Phys. 8, 215 (1975); A. J. Berlinsky, James F. Carolan, and Larry Weiler, Solid State Commun. 15, 795 (1974); F. Herman (unpublished) finds $W = 0.3–0.4$ eV from calculations of the TCNQ dimer.

[42]D. J. Scalapino, Y. Imry, and P. Pincus, Phys. Rev. B 11, 2042 (1975); S. Barišić and K. Uzelac, J. Phys. (Paris) 36, 1267 (1975).

[43]M. J. Rice, Aspen Workshop on 1D Conductors, Aspen, Colo. (July, 1975). P. A. Lee, Aspen Workshop on 1D Conductors, Aspen, Colo. (July, 1975).

[44]The Coulomb interaction between two neighboring chains with charge-density waves, $\rho_i = \rho_0 \cos\varphi_i$ on each may be written

$$U_{\text{interchain}} = \frac{1}{4\epsilon_\perp} \rho_0^2 [2K_0(2k_F d)] \cos(\varphi_i - \varphi_j)$$

where $\epsilon_\perp$ is the perpendicular static dielectric constant, $K_0(x)$ is the complete elliptic integral of the first kind,

and $d$ is the interchain spacing. For $x \gg 1$, $2K_0(x) \simeq (\pi/2x)^{1/2} e^{-x}$. For a more elaborate calculation see K. Saub, S. Barišić, and J. Friedel, Phys. Lett. A 56, 302 (1976).

[45]A. J. Epstein, S. Etemad, A. F. Garito, and A. J. Heeger, Solid State Commun. 9, 1803 (1971); Phys. Rev. B 5, 952 (1971).

[46]S. K. Khanna, A. A. Bright, A. F. Garito, and A. J. Heeger, Phys. Rev. B 10, 2139 (1974).

[47]P. M. Chaikin, A. F. Garito, and A. J. Heeger, Phys. Rev. B 5, 4966 (1972); J. Chem. Phys. 58, 2336 (1973).

[48]T. Moriya, J. Phys. Soc. Jpn. 18, 516 (1963).

[49]D. Jerome, W. Muller, and M. Weger, J. Phys. Lett. (Paris) 35, L77 (1974).

[50]P. M. Horn and D. Rimar, Phys. Rev. Lett. 36, 809 (1976).

[51]A. J. Berlinsky, T. Tiedji, J. F. Carolan, L. Weiler, and W. Freisen, Bull. Am. Phys. Soc. 20, 465 (1975).

[52]M. B. Salamon, J. W. Bray, G. de Pasquali, R. A. Craven, G. Stucky, and A. Schultz, Phys. Rev. B 11, 619 (1975).

[53]P. M. Chaikin, J. F. Kwak, T. E. Jones, A. F. Garito, and A. J. Heeger, Phys. Rev. Lett. 31, 601 (1973); J. F. Kwak, P. M. Chaikin, A. A. Russel, A. F. Garito, and A. J. Heeger, Solid State Commun. 16, 729 (1975).

[54]P. M. Chaikin, R. L. Greene, S. Etemad, and E. M. Engler, Phys. Rev. B 13, 1627 (1976).